

Supplementary Information

Title: Bright” and “Dark” Excited States of an Alternating AT Oligomer Characterized by Femtosecond Broadband Spectroscopy

Authors Wai Ming Kwok,^{*,†} Chensheng Ma^{*,‡} and David Lee Phillips^{*,‡}

[†]*Department of Applied Biology and Chemical Technology, The Hong Kong*

[‡]*Polytechnic University, Hung Hom, Kowloon, Hong Kong, China and Department of Chemistry, The University of Hong Kong, Pokfulam Road, Hong Kong, China*

Journal: *Journal of Physical Chemistry B*

Figure 1S Melting curve of d(AT)₁₀ in the pH6.85 buffered aqueous solution S2

Figure 2S Overview of the TRF spectra obtained for an equal molar A+T mixture with 267 nm photo-excitation S2

Figure 3S Overview of the TRF spectra obtained for d(AT)₁₀ with 267 nm photo-excitation S2

Figure 4S Overview of the TA spectra obtained for an equal molar A+T mixture with 267 nm photo-excitation S3

Figure 5S Overview of the TA spectra obtained for d(AT)₁₀ with 267 nm photo-excitation S3

Figure 6S Examples of fs-TA and fs-TRF spectra of Ado and dT used for the decomposition of the correlated transient A+T spectra. S4

Figure 7S Time dependence of TA and TRF for A+T mixture at various wavelengths and related descriptions. S5

Table 1S Time-constants and weighting factors resulted from dynamic fitting of the TA and TRF time-dependence data in Figure 7S. S5-6

Figure 8S Time dependence of TA and TRF for d(AT)₁₀ at various wavelengths and related illustration. S6

Table 2S Weighting factors resulted from global fittings of the TA and TRF time-dependence data in Figure 8S. S7

Figure 9S Log-normal fitting of the representative transient TRF spectra of d(AT)₁₀. S7

Table 3S Spectral parameters obtained from log-normal simulations of the UV-Vis absorption and the three fluorescence components of d(AT)₁₀. S8

References S8

Figure 1S Melting curve of d(AT)₁₀ in the pH 6.85 buffered aqueous solution

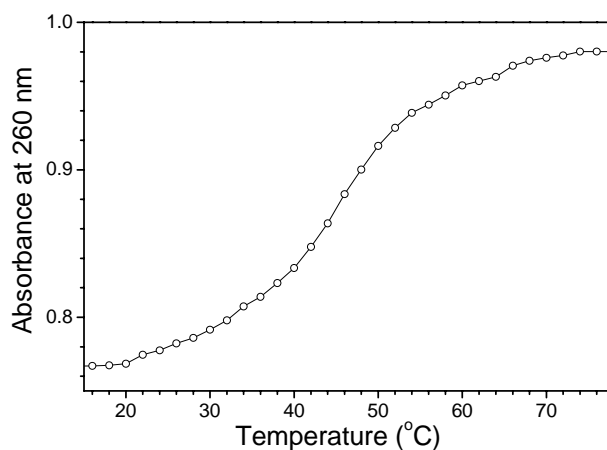


Figure 2S Overview (a) and 50 times enlarged ((b) for delay time from 1.4 ps to 3.75 ps)
TRF spectra obtained for equal molar A+T mixture with 267 nm excitation

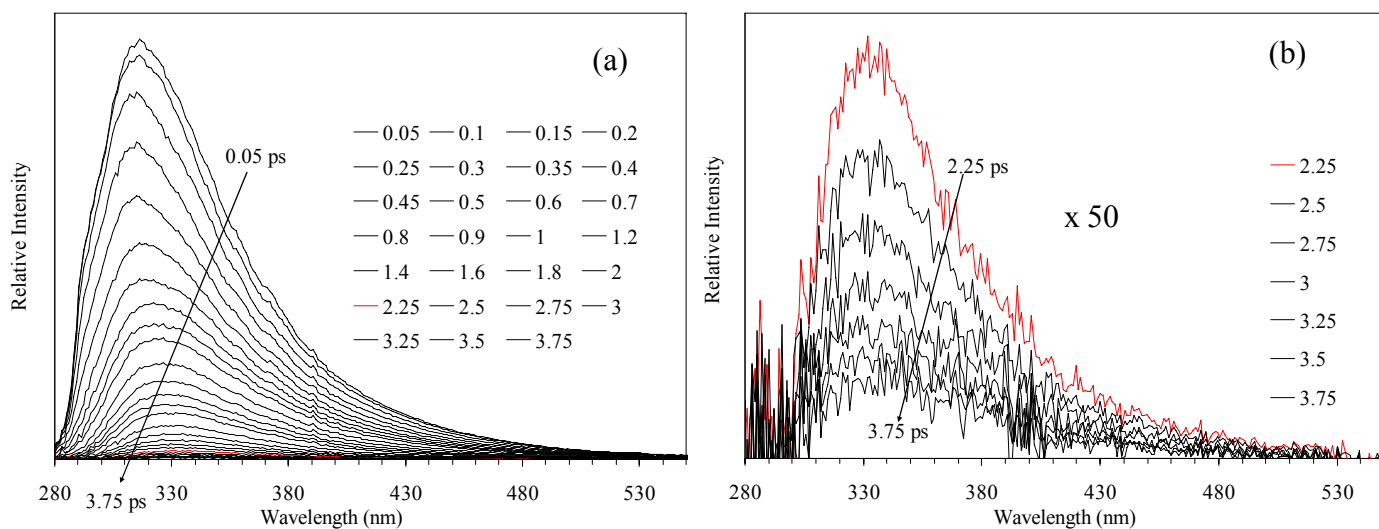


Figure 3S Overview (a) and 23 times enlarged ((b) for delay time from 1.4 ps to 250 ps)
TRF spectra obtained for d(AT)₁₀ with 267 nm excitation

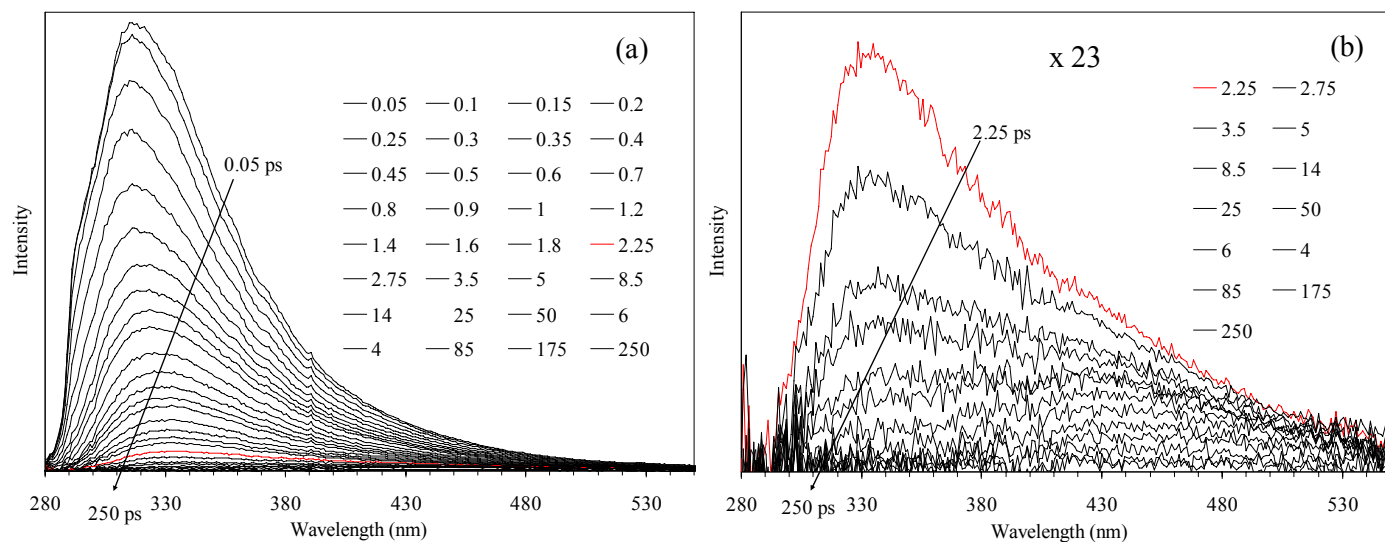


Figure 4S Overview of the TA spectra obtained for A+T mixture with 267 nm excitation

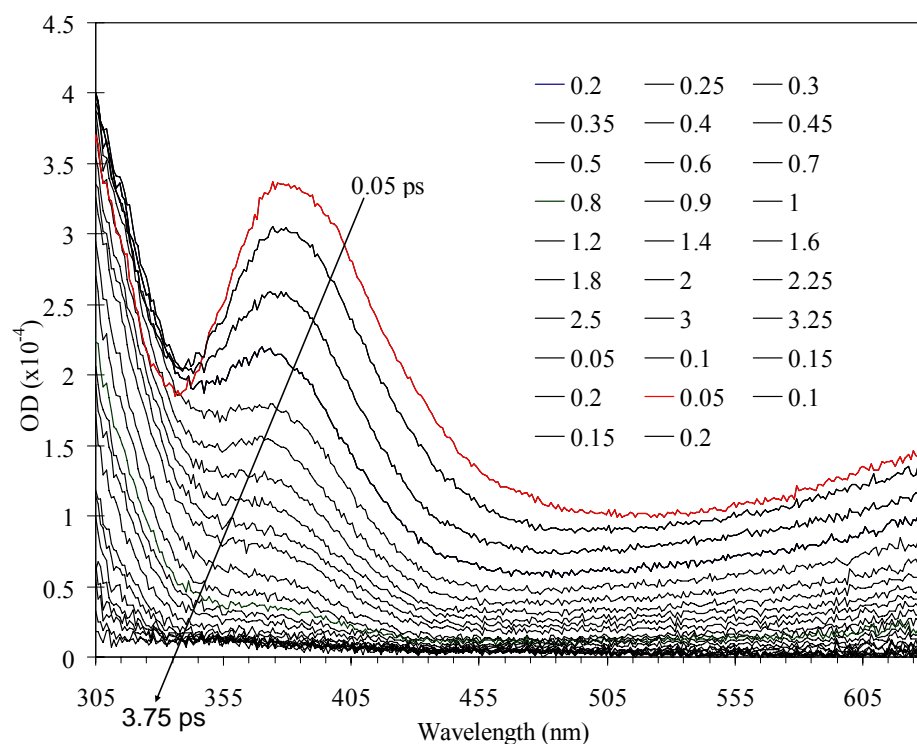


Figure 5S Overview of the TA spectra obtained for d(AT)₁₀ with 267 nm excitation

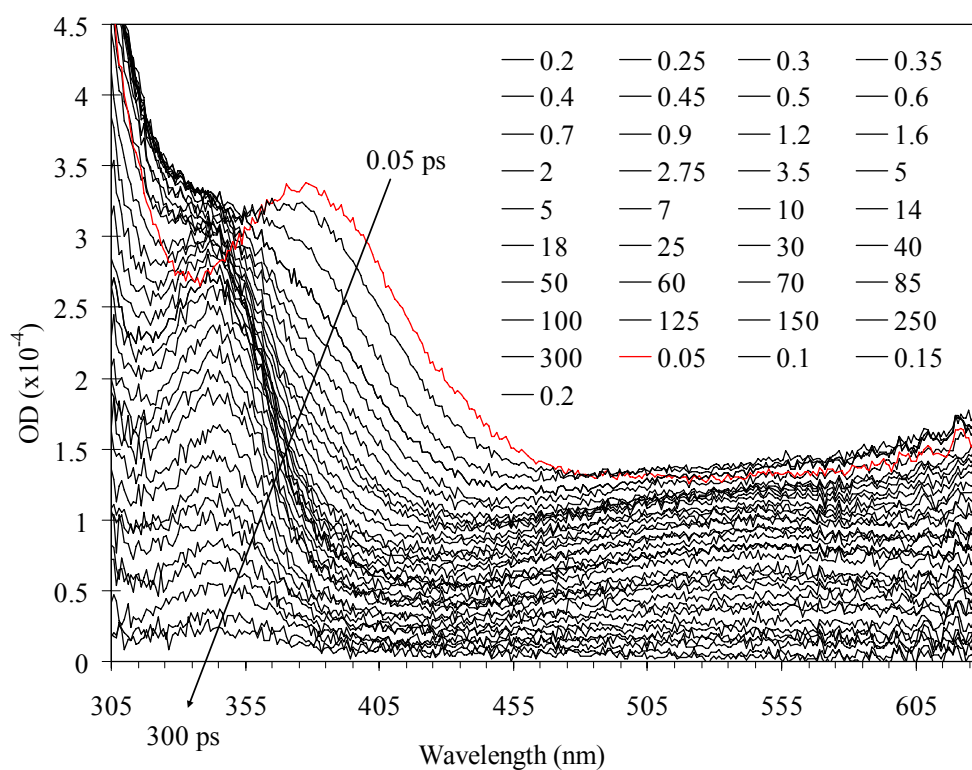


Figure 6S Examples of fs-TA (a, b) and fs-TRF (c, d) spectra of Ado^[1] and dT^[2] obtained under similar experimental conditions as those for the A+T and d(AT)₁₀ measurements herein. After weighted by the absorption proportional factors (0.54 for Ado and 0.46 for dT), these spectra were used to decompose the TA and TRF transient spectra of the corresponding time delays recorded for the A+T mixture (Figure 1 in the main text). It is worthwhile to note the distinct spectral and dynamics features displayed, respectively, by the Ado and dT spectra.

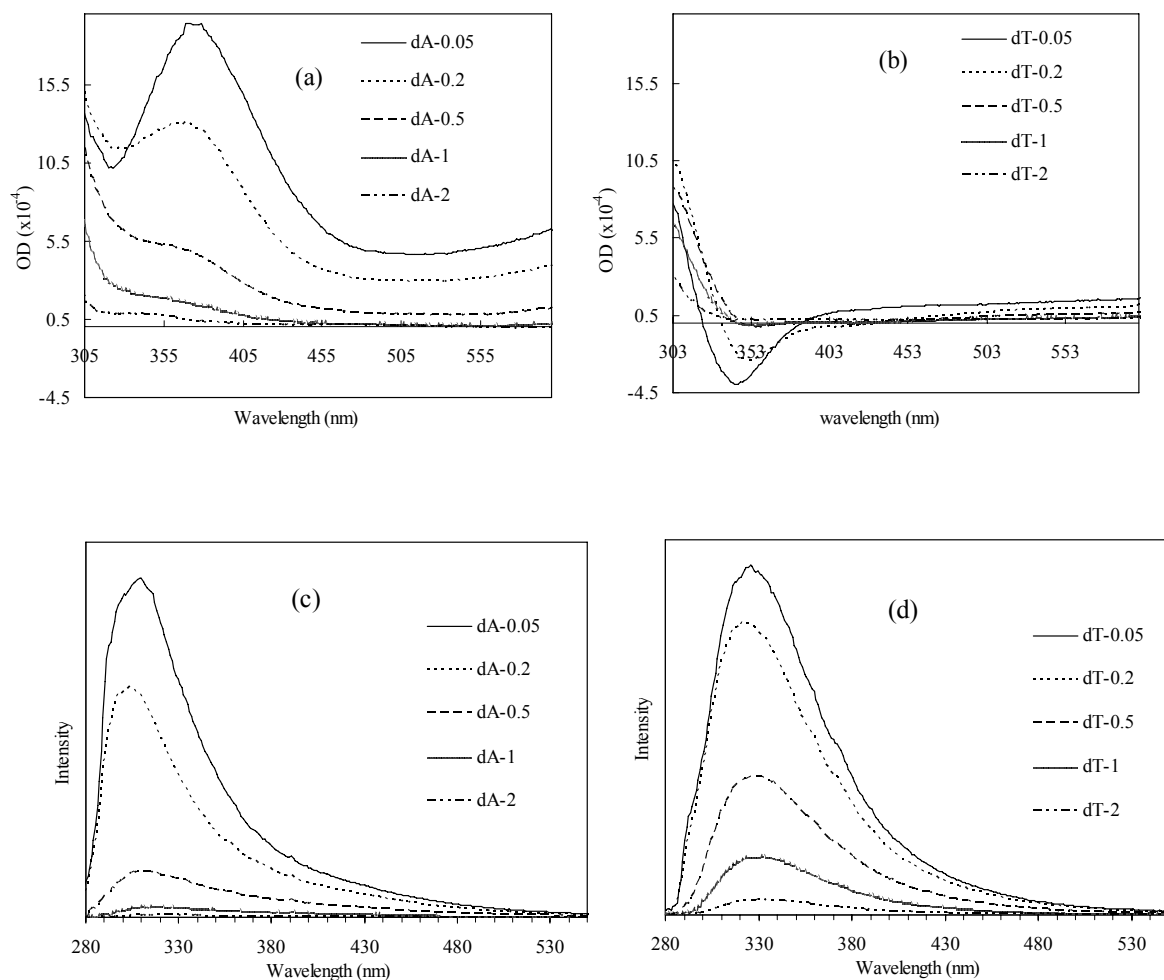
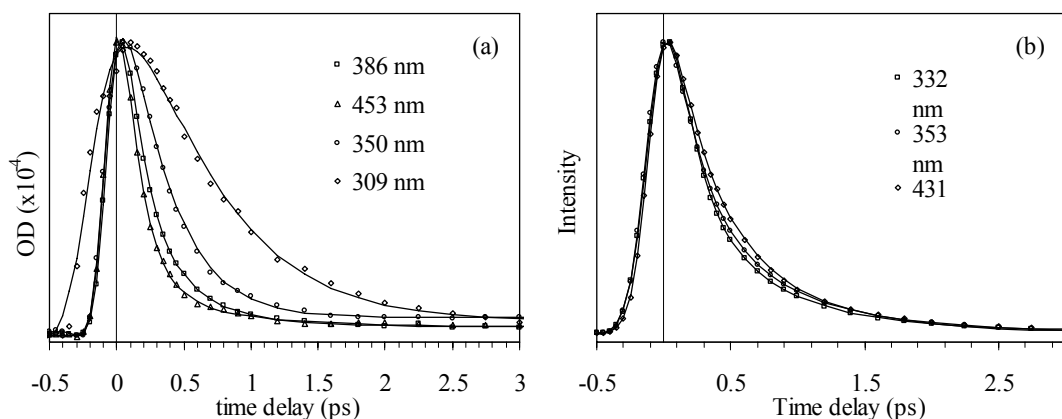


Figure 7S Normalized time dependence of TA (a) and TRF (b) for A+T mixture at various indicated wavelengths resulted from the TA and TRF spectra in Figure 2, Figure 1S and 3S. The data points are from the experimental measurements and solid lines represent kinetic fittings resulted from simulation by using two exponential functions ($a_1\exp(-t/\tau_1) + a_2\exp(-t/\tau_2)$) convoluted with the IRF of the TA or TRF measurements.



For all the fittings, the resulted two time constants are similar, ~ 0.13 – 0.22 ps for τ_1 and ~ 0.46 – 0.74 ps for τ_2 , but associated with different weighting factors (a_1 , a_2) depending on the wavelength examined. For the time profiles shown in the figure, the associated fitting time-constants and weighting factors are listed below in **Table 1S**

Table 1S Fitting parameters for the time-dependences of TA and TRF results displayed in Figure 6S. The χ^2 stands for the Mean Square Deviation of the fittings. All the time profiles are normalized to 1 before the fittings.

TA						
	τ_1 (ps)	a_1	τ_2 (ps)	a_2	a_3	χ^2 ($\times 10^{-5}$)
350 nm ^a	0.14	0.52	0.46	0.46	0.03	9.0
386 nm	0.17	0.82	0.46	0.18		2.5
453 nm	0.15	0.92	0.67	0.08		6.5

TRF					
	t_1 (ps)	a_1	t_2 (ps)	a_2	χ^2 ($\times 10^{-5}$)
332 nm	0.18	0.73	0.69	0.27	0.9
353 nm	0.22	0.69	0.74	0.31	0.8
431 nm	0.22	0.47	0.58	0.53	1.5

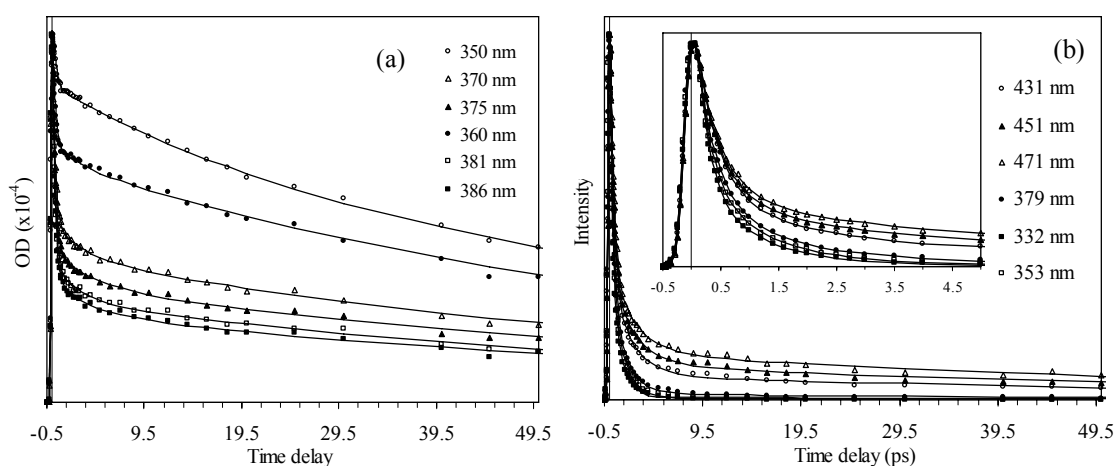
^aThe a_3 value corresponds to the contribution of the residual signal at time delay > 3 ps at this particular wavelength. The signal has been associated with absorption from dT triplet as discussed in the main text.

The excited-state decays of A[•]do and dT are both featured by two exponential dynamics due to involvement of two excited-states, i.e., the L_a ($\pi\pi^*$) and L_b ($\pi\pi^*$) for

Ado^[1] and $\pi\pi^*$ and $n\pi^*$ for dT.^[2] The correlated two time constants are similar but slightly slower for dT than Ado (0.13 ps and 0.45 ps for Ado; 0.15 ps and 0.76 ps for dT).^{2,6} This plus the different spectral characters of the Ado and dT TA and TRF spectra (Figure 6S) account for the wavelength dependent two exponential decays of the TA and TRF results shown in the above figures.

The distinctive TA profile at ~ 309 nm (Figure 6S(a)) that shows a substantial long ~ 0.9 ps decay is due to the additional repopulation of the S_0 by the prompt excited-state IC deactivations and the ensuing cooling of this vibrationally hot S_0 .^[1,2,3] The IC dumps most of the absorbed 267 nm photo-energy into the just recovered S_0 molecules making them vibrationally highly excited and they consequently exhibit a transient absorption at wavelengths slightly beyond the red-edge of their thermal equilibrium S_0 absorption (Figure 1 S).^[3,4] The hot S_0 molecules then gradually transfer the excess vibrational energy into the surrounding medium to re-establish the thermal equilibrium with the surrounding environment. For nucleobases, such a vibrational cooling (VC) process is signified by the wavelength dependent TA decay profiles at a wavelength region below ~ 330 nm and crossing the lowest S_0 absorption band. The slower 309 nm TA decay seen here (correlated with a ~ 0.9 ps time constant) is an indication of the VC process of the 267 nm excited A+T; The TA dynamics at the other longer wavelengths (Figure 6S(a)) and the TRF profiles (Figure 6S(b)) are due to relaxation and deactivation dynamics of Ado and dT excited-states.

Figure 8S Normalized time dependence of TA (a) and TRF (b) for the d(AT)₁₀ at various indicated wavelengths obtained from the TA and TRF spectra in Figure 3, Figure 2S and 4S.



The data points are from the experimental measurements and solid lines represent kinetic fittings from simulation using three exponential function ($a_1\exp(-t/\tau_1) + a_2\exp(-t/\tau_2) + a_3\exp(-t/\tau_3)$) convoluted with the IRF of the TA or TRF measurements.

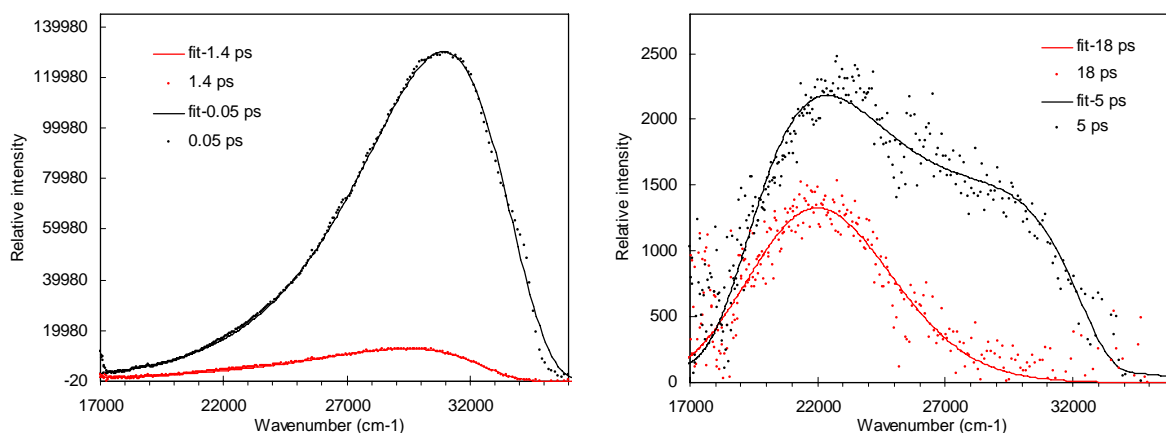
The insert in (b) shows the corresponding dynamics at early time delays. The fittings for the TA and TRF dynamics result in the similar set of time constants, that is 0.3 ± 0.03 ps for the τ_1 , 3.0 ± 0.5 ps for the τ_2 and 72 ± 2 ps for the τ_3 , for the three exponential components but with varying weighting factors depending on the wavelength examined. The weighting factors resulted for each of the fittings displayed in Figure 7S(a) and (b) are listed in **Table 2S** as the following.

Table 2S Fitting parameters for the time-dependences of TA and TRF results displayed in Figure 7S. The χ^2 stands for the Mean Square Deviation of the fittings. All the time profiles are normalized to 1 before the fittings.

TA				
	a_1	a_2	a_3	$\chi^2 (x10^{-5})$
386 nm	0.784	0.064	0.152	3.9
350 nm	0.255	0.064	0.681	16.4
370 nm	0.661	0.071	0.268	6.6
375 nm	0.732	0.066	0.202	4.5
360 nm	0.494	0.038	0.468	11.0
381 nm	0.757	0.069	0.174	2.8

TRF				
	a_1	a_2	a_3	$\chi^2 (x10^{-5})$
471 nm	0.731	0.178	0.091	2.7
451 nm	0.746	0.187	0.067	1.9
431 nm	0.749	0.204	0.046	1.1
379 nm	0.755	0.234	0.011	0.9
353 nm	0.743	0.253	0.004	1.1
332 nm	0.823	0.176	0.002	5.7

Figure 9S Log-normal fitting of the representative transient TRF spectra of d(AT)₁₀. The 5 ps transient spectrum was simulated by weighted superposition of the S_G and S_E spectra that was obtained from fitting of the 1.4 ps and 18 ps experimental spectra, respectively.



The log-normal function follows:

$$F(\nu) = h \begin{cases} \exp[-\ln(2)\{\ln(1+\alpha)/\gamma\}^2] & \alpha > -1 \\ 0 & \alpha \leq -1 \end{cases} \dots\dots\dots(\text{eq 1})$$

$$\alpha \equiv 2\gamma(\nu - \nu_p)/\Delta$$

Where h is the peak height, ν_p the peak frequency, γ the asymmetry parameter and Δ the width parameter are adjusted to simulate the spectral profile of a fluorescence or absorption spectrum.

Table 3S Spectral parameters obtained by log-normal simulation of the UV-Vis absorption and the three fluorescence component spectra (the 0.05 ps, 1.4 ps, and 18ps spectra in Figure 3 in the main text) of d(AT)₁₀ oligomer.

	UV-abs	Transient fluorescence		
		0.05 ps	1.4 ps	20 ps
γ	0.2	-0.4	-0.6	0.3
ν_p (cm ⁻¹)	38110	30910	29428	21820
Δ (cm ⁻¹)	5223	6846	7837	6114
Stokes shift (cm ⁻¹)		7200	8682	16290

References

- [1] W.-M. Kwok, C. Ma, D. L. Phillips, *J. Am. Chem. Soc.* **2006**, *128*, 11894-11905.
- [2] W.-M. Kwok, C. Ma, D. L. Phillips, *J. Am. Chem. Soc.* **2008**, *130*, 5131-5139.
- [3] J. L. Pecourt, J. Peon, B. Kohler, *J. Am. Chem. Soc.* **2001**, *123*, 10370-10378.
- [4] R. J. Sension, S. T. Repinec, R. M. Hochstrasser, *J. Chem. Phys.* **1990**, *93*, 9185-9188.